Error Calibration on Five-axis Machine Tools by on-the-machine Measurement of Artifacts using a Touch-trigger Probe

Soichi IBARAKI[1], Takeyuki IRITANI[1] and Tetsuya MATSUSHITA[2]
[1] Department of Micro Engineering, Kyoto University, Japan, ibaraki@prec.kyoto-u.ac.jp (Ibaraki)
[2] Okuma Corporation

Abstract:
As a basis to improve the motion accuracy of five-axis machining centers, it is important to develop a methodology to measure it in an accurate, efficient, and automated manner. This paper proposes a scheme to calibrate error motions of rotary axes by on-the-machine measurement of artifacts by using a contact-type touch-trigger probe installed on the machine's spindle. Location errors, defined in ISO 230-7, of rotary axes are the most fundamental error factors in the five-axis kinematics. A larger class of error motions can be modeled as geometric errors that vary depending on the angular position of a rotary axis. The objective of the present scheme is to identify not only geometric errors, but also such position-dependent geometric errors, or "error map," of rotary axes. Its experimental demonstration is presented.
Keywords: Five-axis machine tools, location errors, position-dependent geometric errors, touch-trigger probe, error calibration.

1. Introduction

Machine tools with two rotary axes to tilt and rotate a tool and/or a workpiece, in addition to three orthogonal linear axes, are collectively called five-axis machine tools. With the recent rapid popularization of five-axis machining centers, the improvement of their motion accuracies is crucial demand in the manufacturing market.

As a basis to improve the motion accuracy of five-axis machines, it is important to develop a methodology to measure it in an accurate, and efficient manner. ISO 10791-1[1] to -3 standards describe no-load or quasi-static measurements with the main focus on evaluating static position and orientation errors of the axis average line of a rotary axis. Such errors are called location errors in ISO 230-7 [2], or geometric errors [3]. The importance of location errors is well understood by many machine tool manufactures, as one of the most fundamental error factors in the five-axis kinematics. There has been many research works reported in the literature on the identification of location errors. Typical ones include the application of the telescoping double ball bar (DBB) [3,4,5]. Its inclusion in the revision of ISO 10791-6 is currently under the discussion at ISO TC39/SC2 [6,7].

In today's commercial CNCs for machine tools, it is common to compensate various static error motions of a linear axis by modifying the command position based on a pre-calibrated error map [8]. Analogous compensation of static error motions, location errors in particular, of a rotary axis is possible, and has been demonstrated in the literature [9,10]. To meet the market's demand for higher motion accuracy of a five-axis machining center, such a compensation may be crucial in near future. To implement it on mass-produced commercialized machines, it is crucial to perform high-efficient, and *automated* error calibration to all machines by a machine tool builder. Although ball bar measurements for five-axis machines are already accepted by some machine tool builders, they requires at least a couple of setup changes by an experienced operator to identify all location errors. Its full automation is therefore very difficult in practice.

This paper proposes a scheme to calibrate error motions of rotary axes by on-the-machine measurement of artifacts by using a contact-type touch-trigger probe installed on the machine's spindle. In recent years, high-accuracy touch-trigger probes for machine tools, which typically have one-directional measurement repeatability smaller than 1 μm, are available from some vendors. ISO TC39/SC2 have been also discussing the standardization of test code for measuring performance of such a touch-trigger probe (ISO/DIS 230-10 [11]). From its nature, a touch-trigger probe must have a good communication with a CNC system, which potentially facilitates the automation of error calibration and compensation generation processes.

Some latest commercial CNCs have the capability to perform an error calibration of a rotary table by using a touch-trigger probe. It is, however, typically limited to the identification of the center (and possibly the orientation) of a rotary table. The center and the orientation of a rotary table is a part of its location errors. More recent research works presented a probe-based scheme to calibrate all location errors of rotary axes [12,13].

A larger class of more complex error motions of rotary axis, such as the gravity deformation, angular positioning error, pure radial error motions or tilt error motions of a rotary axis, can be modeled as location errors that vary depending on the angular position of a rotary axis. The objective of this paper is to present a error calibration scheme based on on-the-machine measurement by a touch-trigger probe to identify not only location errors, but also such position-dependent geometric (location) errors. Its experimental demonstration on a commercial five-axis machining center of a tilting rotary table configuration will be presented.

Table 1: Descriptions of position-dependent geometric errors associated with rotary axis

Symbol	Symbol	Description
$\alpha_{AY}(A)$	EAA	Angular error of A-axis rotation
$\beta_{AY}(A)$	EBA	Orientation changes of A-axis around Y-axis with A rotation
$\gamma_{AY}(A)$	ECA	Orientation changes of A-axis around Z-axis with A rotation
$\alpha_{CA}(A,C)$	EAC	Orientation changes of C-axis around C-axis with A, C rotation
$\beta_{CA}(A,C)$	EBC	Orientation changes of C-axis around Y-axis with A, C rotation
$\gamma_{CA}(A,C)$	ECC	Angular error of C-axis rotation
$\delta x_{AY}(A)$	EXA	Location changes of A-axis center in X-direction with A rotation
$\delta y_{AY}(A)$	EYA	Location changes of A-axis center in Y-direction with A rotation
$\delta z_{AY}(A)$	EZA	Location changes of A-axis center in Z-direction with A rotation
$\delta x_{CA}(A,C)$	EXC	Location changes of C-axis center in X-direction with A, C rotation
$\delta y_{CA}(A,C)$	EYC	Location changes of C-axis center in Y-direction with A, C rotation
$\delta z_{CA}(\mathbf{A,C})$	EZC	Location changes of C-axis center in Z-direction with A, C rotation

2. Error Parameters to be Identified in Five-axis Kinematic Model

2.1 Machine Configuration

This paper considers a 5-axis machine configuration with a titling rotary table (driven by A- and C-axes) depicted in Fig. 1. It must be emphasized that the basic idea of this paper can be straightforwardly extended to any other configurations of five-axis machines.

2.2 Position-dependent Geometric Errors

Location errors, defined in ISO 230-7 [2], only represent *mean* position and orientation of a rotary axis. The location and orientation of a rotary axis may vary due to its rotation (described by the term "axis of rotation error motion" in ISO 230-7 [2]). By parameterizing location errors as a function of angular position of rotary axis, a larger class of axis of rotation error motions can be described (see [14] for further details). They are referred to as position-dependent geometric errors in this paper.

Table 1 shows position-dependent geometric errors for the machine configuration in Fig. 1. The objective of the scheme presented in this paper is to identify all position-dependent geometric errors shown in Table 1. It is to be noted that parameters associated with B-axis are dependent only on the angular position of B-axis, while those associated with C-axis are dependent on both B- and C-axis angular positions. This is because an error motion of C-axis may be affected by B-axis angular position (its typical causes include gravity-induced deformation of bearings or mechanical structure).

To eliminate the redundancy in the influence of geometric errors of A- and C-axes on the tool center position, geometric errors of C-axes are defined such that:

$$\sum_{j=1}^{N_c}\delta x_{CA}(A_i,C_j)=\sum_{j=1}^{N_c}\delta y_{CA}(A_i,C_j)=\sum_{j=1}^{N_c}\delta z_{CA}(A_i,C_j)=0$$
$$\sum_{j=1}^{N_c}\alpha_{CA}(A_i,C_j)=\sum_{j=1}^{N_c}\beta_{CA}(A_i,C_j)=\sum_{j=1}^{N_c}\gamma_{CA}(A_i,C_j)=0 \quad (1)$$

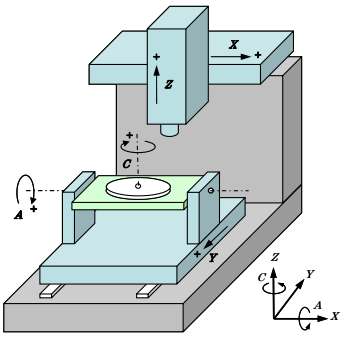

Figure 1: Machine configuration.

It is also important to note that this paper assumes that error motions of linear axes are negligibly small compared to those of a rotary axis.

2.3 Kinematic Modeling of Five-axis Machine

The kinematic model to compute the tool center position with respect to the workpiece is the basis of the error calibration presented in the following sections. Since five-axis kinematic models can be found in many previous publications [15], this subsection only briefly reviews it.

Define the *reference coordinate system* as the coordinate system fixed to the Y-axis frame. This coordinate system is independent of A- and C-rotations. Suppose that the tool center location in the reference coordinate system is given by ${}^{r}p\in\Re^3$. The left-side superscript *r* represents a vector in the reference coordinate system.

Define the *workpiece coordinate system* as the coordinate system attached to the rotary table. The homogeneous transformation matrix (HTM) representing the transformation from the workpiece coordinate system to the reference coordinate system is given by:

$${}^{r}T_w={}^{r}T_a\,{}^{a}T_c \quad (2)$$

where

$$\begin{aligned}{}^{r}T_a &= D^1(\delta x_{AY}(A))D^2(\delta y_{AY}(A))D^3(\delta z_{AY}(A))\\ &\quad D^4(\alpha_{AY}(A))D^5(\beta_{AY}(A))D^6(\gamma_{AY}(A))D^4(A)\\ {}^{a}T_c &= D^1(\delta x_{CA}(A,C))D^2(\delta y_{CA}(A,C))D^3(\delta z_{CA}(A,C))\\ &\quad D^4(\alpha_{CA}(A,C))D^5(\beta_{CA}(A,C))D^6(\gamma_{CA}(A,C))D^6(C)\end{aligned} \quad (3)$$

and *A* and *C* respectively represent the command angular position of A and C axes. $D^1(x)$, $D^2(y)$, $D^3(z)\in\Re^{4\times4}$ respectively represent the HTM for linear motions in X-, Y-, and Z-directions by distances *x*, *y*, and *z*. $D^4(a)$, $D^5(b)$, $D^6(c)\in\Re^{4\times4}$ respectively represent the HTM for angular motions about X, Y and Z axes by angles *a*, *b*, and *c*. See e.g. [15] for the formulation of each HTM.

Hence, the tool center location in the workpiece frame, ${}^{w}p\in\Re^3$, can be given as follows. Note that the left-side superscript *w* denotes the vector defined in the workpiece coordinate system.

$$\begin{bmatrix}{}^{w}p\\1\end{bmatrix}=({}^{r}T_w)^{-1}\begin{bmatrix}{}^{r}p\\1\end{bmatrix} \quad (4)$$

2.4 Measuring Instrument

This paper uses a typical commercial contact-type

touch-trigger probe to be installed on a machine spindle. The probe is approached to the object surface in the direction normal to it. When the contact of a probe ball with the object is detected, a signal is sent to a CNC to stop the drive and record its position in the global coordinate system. The position of the contact point on the surface, p, is calculated from the machine position, the approaching direction and the calibrated ball radius. According to the probe software's standard procedure, the pre-travel variation for different approaching directions is compensated based on its pre-calibration.

3. Measurement Procedure

First, A and C angular positions, A_i and C_j (i=1~N_a, j=1~N_c), where position-dependent geometric errors are to be identified, must be determined. For example, in the experimental case study to be presented in Section 5, considering the maximum stroke of each rotary axis, they are set at A_i =0°, -30°, -60°, -90° (N_a=4). and C_j =0°, 60°, 120°, 180°, 240°, 300° (N_c =6). At each combination of A_i and C_j (total $N_a \times N_c$=24 positions), the following measurement procedure is performed:

Three artifacts of a square column geometry are fixed on the machine's rotary table as shown in Fig. 2. At A_i=C_j=0°, total 15 points on three artifacts are measured as shown by circles. When A_i, C_j ≠0°, to avoid unwanted interference of the probe to artifacts, less points are probed. For example, Fig. 3 shows probed points for (a) A_i=0°, C_j=0°, (b) A_i=0°, C_j=60° and (c) A_i=-90°, C_j=0°. The index k labels probed points (k=1~18).

For indexed angles A_i and C_j, the reference location of the probed point k is represented by $\tilde{p}(i, j, k) \in \Re^3$. Its measured position by a touch-trigger probe is represented by $p(i, j, k) \in \Re^3$.

Note that multiple artifacts are used to magnify the influence of an angular (tilt) error of rotary axis in measured displacements. For example, as illustrated in Fig. 4, the angular positioning error of C-axis, γ_{CA}, affects the Y-position of probed points by:

$$y_2 - y_1 = L_1 \gamma_{CA} \tag{5}$$

The influence of the measurement uncertainty in y_1 and y_2 to the identification of γ_{CA} becomes smaller when L is larger. By using two artifacts, we can have larger L without using larger artifact. Considering the symmetry of artifact locations in both X and Y directions, we used three artifacts as shown in Fig. 2.

4. An Algorithm to Identify Position-dependent Geometric Errors

4.1 Calculation of Table Position and Orientation

The objective of the present algorithm is to identify position-dependent geometric errors of A- and C-axes shown in Table 1 for A_i and C_j (i=1~N_a, j=1~N_c) from probed positions, $p(i, j, k)$ (k=1~N_k).

For indexed angles A_i and C_j, represent the position error of the rotary table from its nominal position in X, Y, and Z directions of the global coordinate system by ($\Delta x(i, j)$, $\Delta y(i, j)$, $\Delta z(i, j)$). Represent its orientation error around X, Y, and Z directions of the global coordinate system by

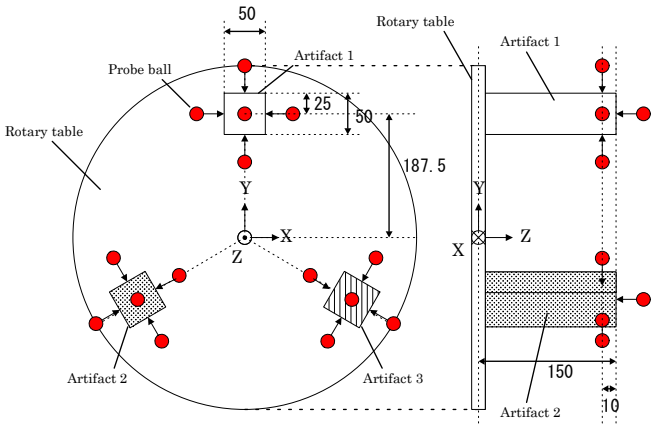

Figure 2: Position of measured points on the artifacts. (C=0°,A=0°).

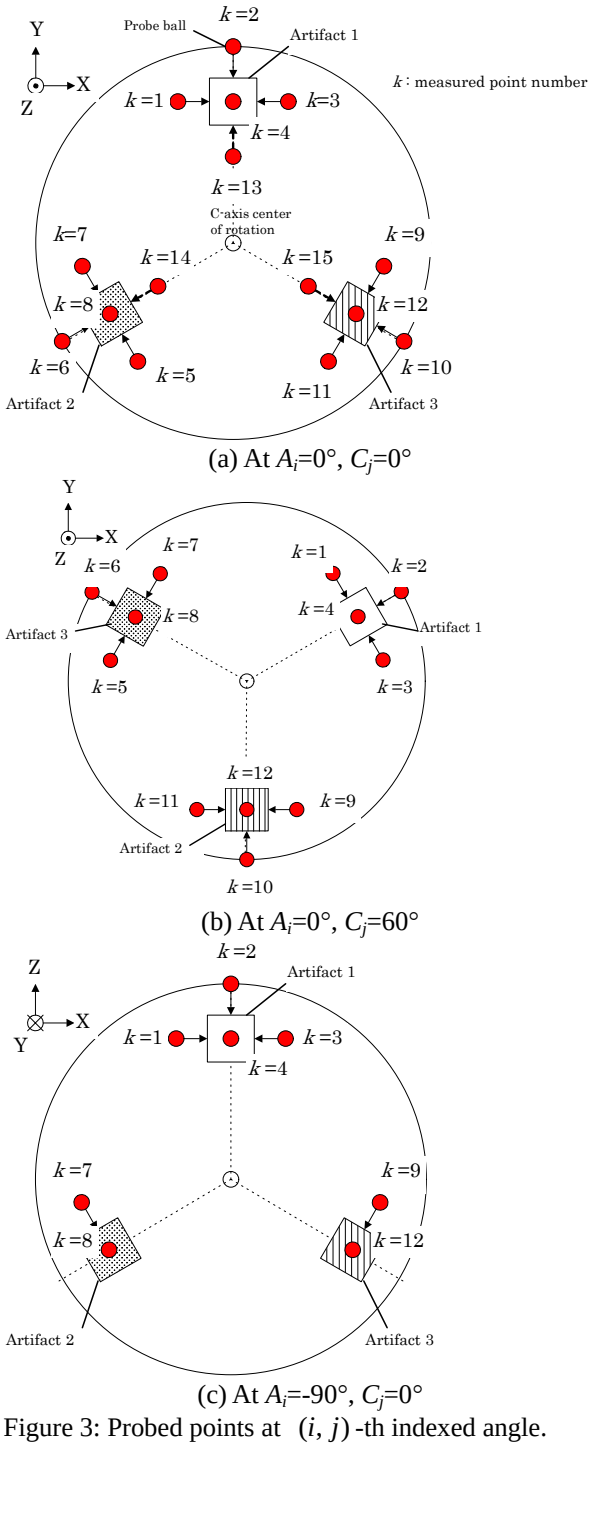

Figure 3: Probed points at (i, j) -th indexed angle.

($\Delta a(i,j)$, $\Delta b(i,j)$, $\Delta c(i,j)$). First step of the algorithm is to calculate $\Delta x(i,j)$~$\Delta c(i,j)$ from probed positions, $p(i,j,k)$.

When A_i=C_j=0° (i=j=1), measured points, $p(1,1,k)$ (k=1~N_k), represent the location, orientation, and geometry of three artifacts. By rotating it by A_i and C_j, $p(1,1,k)$ is moved to $p_1(i,j,k)$ by:

$$p_1(i,j,k) = D^4(A_i)D^6(C_j)\,p(1,1,k) \tag{6}$$

It must be noted that a touch-trigger probe is sensitive only to the displacement of the probed point in its approaching direction. For the k-th point, suppose that the approaching direction is given by a unit vector $\tilde{n}(i,j,k) \in \Re^3$. Then, the table position and orientation at A_i and C_j, namely $\Delta x(i,j)$~$\Delta c(i,j)$, are computed by solving the following minimization problem:

$$\min \sum_{k=1}^{N_k} \Big[\big\{ p(i,j,k) - D^1(\Delta x(i,j))D^2(\Delta y(i,j))D^3(\Delta z(i,j)) \\ D^4(\Delta a(i,j))D^5(\Delta b(i,j))D^6(c(i,j))\,p_1(i,j,k) \big\} \cdot \tilde{n}(i,j,k) \Big]^2 \tag{7}$$

This minimization problem can be approximated as a linear programming problem as follows:

When Δx, Δy, Δz, Δa, Δb, and Δc are sufficiently small, the following approximation generally holds:

$$D^1(\Delta x)D^2(\Delta y)D^3(\Delta z)D^4(\Delta a)D^5(\Delta b)D^6(\Delta c) \cong \begin{bmatrix} 1 & -\Delta c & \Delta b & \Delta x \\ \Delta c & 1 & -\Delta a & \Delta y \\ -\Delta b & \Delta a & 1 & \Delta z \\ 0 & 0 & 0 & 1 \end{bmatrix} \tag{8}$$

By using this, Eq. (7) can be approximated by:

$$\min \sum_{k=1}^{N_k} \Big[\big\{ \big(p(i,j,k) - p_1(i,j,k) \big) \\ - \begin{bmatrix} 1 & 0 & 0 & 0 & z_1(i,j,k) & -y_1(i,j,k) \\ 0 & 1 & 0 & -z_1(i,j,k) & 0 & x_1(i,j,k) \\ 0 & 0 & 1 & y_1(i,j,k) & -x_1(i,j,k) & 0 \end{bmatrix} \begin{bmatrix} \Delta x(i,j) \\ \Delta y(i,j) \\ \Delta z(i,j) \\ \Delta a(i,j) \\ \Delta b(i,j) \\ \Delta c(i,j) \end{bmatrix} \big\} \cdot \tilde{n}(i,j,k) \Big]^2 \tag{9}$$

where $p_1(i,j,k)$=$[x_1(i,j,k), y_1(i,j,k), z_1(i,j,k)]^{\mathrm{T}}$. This can be solved by the least square method.

4.2 Calculation of Position-dependent Geometric Errors of Rotary Axes

The table position and orientation at A_j and C_i, $\Delta x(i,j)$~$\Delta c(i,j)$, are then separated into position-dependent geometric errors of A- and C-axes shown in Table 1.

When the nominal position in the global coordinate system is given by ${}^r\tilde{p}$, its actual position under position-dependent geometric errors of A- and C-axes is given based on the kinematic model (4) as follows:

$${}^r p = {}^r T_w \left({}^r \tilde{T}_w \right)^{-1} {}^r \tilde{p} \tag{10}$$

where ${}^r T_w$ is given by Eq. (2) and ${}^r \tilde{T}_w$ is the HTM representing the nominal rotation by A_i and C_j. From this formulation, with the approximation (8), the relationship of the table position and orientation, $\Delta x(i,j)$~$\Delta c(i,j)$, and position-dependent geometric errors of A- and C-axes is formulated as follows:

$$\Delta x(i,j) = \delta x_{AY}(A_i) + \delta x_{CA}(A_i, C_j)$$
$$\Delta y(i,j) = \delta y_{AY}(A_i) + \delta y_{CA}(A_i, C_j)\cos A_i - \delta z_{CA}(A_i, C_j)\sin A_i$$

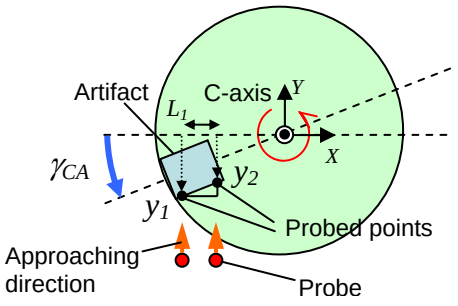

(a) With one artifact.

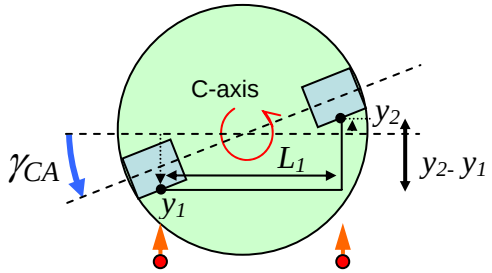

(b) With two artifacts.

Figure 4: Magnification of the influence of orientation errors by using two artifacts

$$\Delta z(i,j) = \delta z_{AY}(A_i) + \delta z_{CA}(A_i, C_j)\cos A_i + \delta y_{CA}(A_i, C_j)\sin A_i$$
$$\Delta a(i,j) = \alpha_{AY}(A_i) + \alpha_{CA}(A_i, C_j) \tag{11}$$
$$\Delta b(i,j) = \beta_{AY}(A_i) + \beta_{CA}(A_i, C_j)\cos A_i - \gamma_{CA}(A_i, C_j)\sin A_i$$
$$\Delta c(i,j) = \gamma_{AY}(A_i) + \gamma_{CA}(A_i, C_j))\cos A_i + \beta_{CA}(A_i, C_j)\sin A_i$$

From the assumption (1), geometric errors of A-axis can be computed by:

$$\delta\hat{x}_{AY}(A_i) = \underset{j}{\mathrm{mean}}\{\Delta x(i,j)\}, \quad \delta\hat{y}_{AY}(A_i) = \underset{j}{\mathrm{mean}}\{\Delta y(i,j)\}$$
$$\delta\hat{z}_{AY}(A_i) = \underset{j}{\mathrm{mean}}\{\Delta z(i,j)\}\cdot \quad \hat{\alpha}_{AY}(A_i) = \underset{j}{\mathrm{mean}}\{\Delta a(i,j)\} \tag{12}$$
$$\hat{\beta}_{AY}(A_i) = \underset{j}{\mathrm{mean}}\{\Delta b(i,j)\}, \quad \hat{\gamma}_{AY}(A_i) = \underset{j}{\mathrm{mean}}\{\Delta c(i,j)\}$$

Then, geometric errors of C-axis are computed by:

$$\begin{bmatrix} \delta\hat{x}_{CA}(A_i,C_j) \\ \delta\hat{y}_{CA}(A_i,C_j) \\ \delta\hat{z}_{CA}(A_i,C_j) \\ 1 \end{bmatrix} = \left\{ D^4(A_i) \right\}^{-1} \begin{bmatrix} \Delta x(i,j) - \delta\hat{x}_{AY}(A_i) \\ \Delta y(i,j) - \delta\hat{y}_{AY}(A_i) \\ \Delta z(i,j) - \delta\hat{z}_{AY}(A_i) \\ 1 \end{bmatrix}$$
$$\begin{bmatrix} \hat{\alpha}_{CA}(A_i,C_j) \\ \hat{\beta}_{CA}(A_i,C_j) \\ \hat{\gamma}_{CA}(A_i,C_j) \\ 1 \end{bmatrix} = \left\{ D^4(A_i) \right\}^{-1} \begin{bmatrix} \Delta a(i,j) - \hat{\alpha}_{AY}(A_i) \\ \Delta b(i,j) - \hat{\beta}_{AY}(A_i) \\ \Delta c(i,j) - \hat{\gamma}_{AY}(A_i) \\ 1 \end{bmatrix} \tag{13}$$

5. Experimental Case Study

The present error calibration scheme is applied to a commercial middle-size 5-axis machining center of the configuration shown in Fig. 1. A touch-trigger probe, RMP-600 by Renishaw, is used in experiments. RMP-600 employs strain gauges to detect the contact of the probe ball, and has the uni-directional repeatability (2σ) of 0.35 μm with the stylus length 100 mm [16]. A ruby sphere of ϕ6 mm is used as a probe ball.

Three artifacts of aluminum alloy A5052 are used. The geometry of artifacts is shown in Fig. 2. Figure 5 shows

Figure 5: Experimental setup.

artifacts fixed on the table. Total 219 points were measured, and total measurement time was about 28 min.

Figure 6 shows measured table positions and orientations, $\Delta x(i, j)$~$\Delta c(i, j)$, calculated from probed positions as presented in Section 4.1. Only (a) A_j=0° and (b) A_j=-90° are shown as examples. To check the repeatability of probing, the test was repeated for three times and all are shown in Fig. 6.

Figure 7 shows position-dependent geometric errors of A-axis identified by the algorithm in Section 4.2. Figure 9 shows position-dependent geometric errors of C-axis. Only those at A_j=0° (i=1) and A_j=-90° (i=4) are shown as examples.

The following observations can be made:

- $\alpha_{AY}(A_i)$ (in Fig. 7(b)) shows that there is relatively larger angular positioning error of A-axis; at maximum 2×10^{-3} deg at A=-90º.
- $\alpha_{CA}(A_i, C_j)$ (in Fig. 8) shows slight tilt error motions of C-axis (within $\pm0.5\times10^{-3}$ deg). No significant influence of A-axis on this tilt error motion is observed.
- No other significant error motions are observed.

Remark:
Since the location and the orientation of artifacts, as well as their geometry, are measured at A_i= C_j=0° as shown in Fig. 3(a), and the table displacement and rotation at other A_i's and C_j's are identified with respect to them, the location, orientation, and geometry of artifacts do not impose significant influence on identified geometric errors.

More complete uncertainty analysis for the present scheme is left for our future research.

6. Concluding Remark

Position-dependent geometric errors identified by the present scheme can be seen as the "error map" of each rotary axis. The algorithm presented in Section 4 focuses on separation of the table's error motion into the error maps of each axis. When the error map of each rotary axis is obtained, its compensation is straightforward.

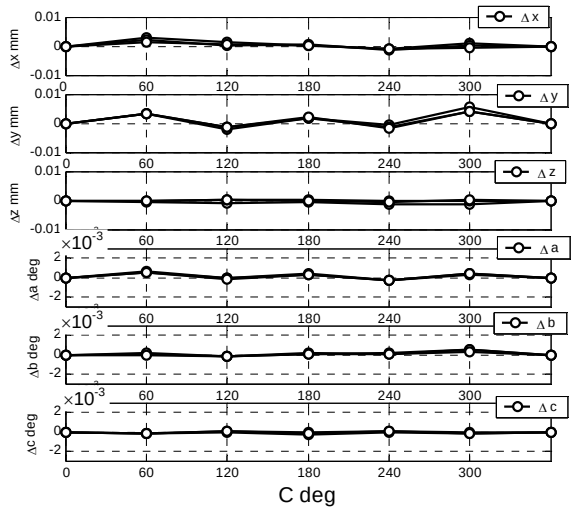

(a) At A_i=0° (i=1).

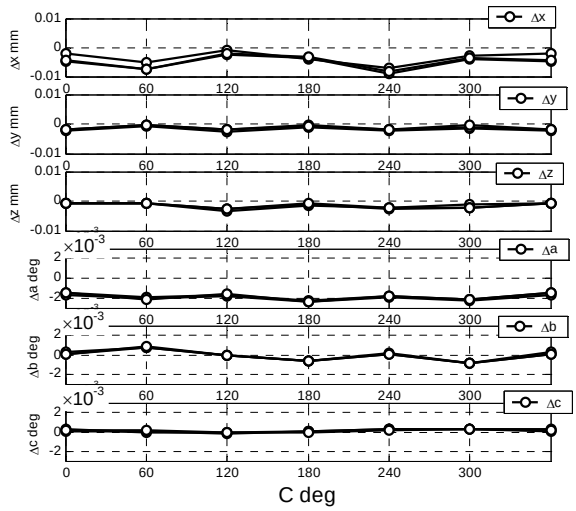

(b) At A_i=-90° (i=4).

Figure 6: Identified table positions and orientations, $\Delta x(i, j)$~$\Delta c(i, j)$ for various C-positions (j=1~7).

References

[1] ISO 10791-1:1998, Test conditions for machining centres -- Part 1: Geometric tests for machines with horizontal spindle and with accessory heads (horizontal Z-axis).

[2] ISO 230-7:2006, Test code for machine tools -- Part 7: Geometric accuracy of axes of rotation.

[3] Abbaszaheh-Mir, Y., Mayer, J. R. R., Clotier, G., Fortin, C., 2002, Theory and simulation for the identification of the link geometric errors for a five-axis machine tool using a telescoping magnetic ball-bar, *Int'l J. of Production Research*, Vol. 40, No. 18, pp. 4781-4797.

[4] Kakino, Y., Ihara, T., Sato, H., Otsubo, H., 1994, A Study on the motion accuracy of NC machine tools (7th report) --Measurement of motion accuracy of 5-axis machine by DBB tests--, *J. of Japan Society for Precision Engineering*, Vol. 60, No. 5, pp. 718--723 (in Japanese).

[5] Tsutsumi, M., Saito, A., 2003, Identification and compensation of systematic deviations particular to 5-axis machining centers, *Int'l J. of Machine Tools and Manufacture*, Vol. 43, pp. 771-780.

[6] Tsutsumi, M., Ihara, Y., Saito, A., Mishima, N., Ibaraki, S., Yamamoto, M., Kobayashi, M., Yonetani, T., 2008, Standardization of testing methods for kinematic motion of five-axis machining centers -- Draft

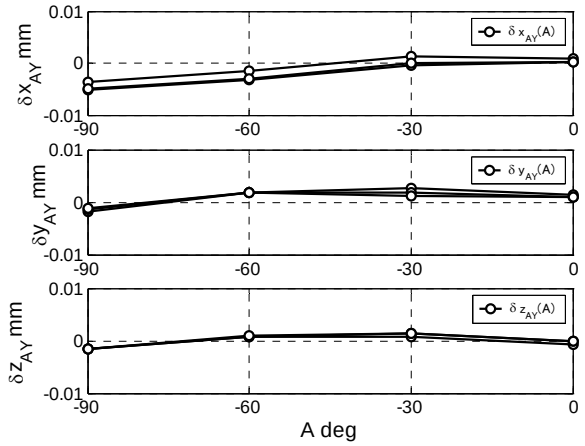

(a) $\delta x_{AY}(A_i)$, $\delta y_{AY}(A_i)$, and $\delta z_{AY}(A_i)$.

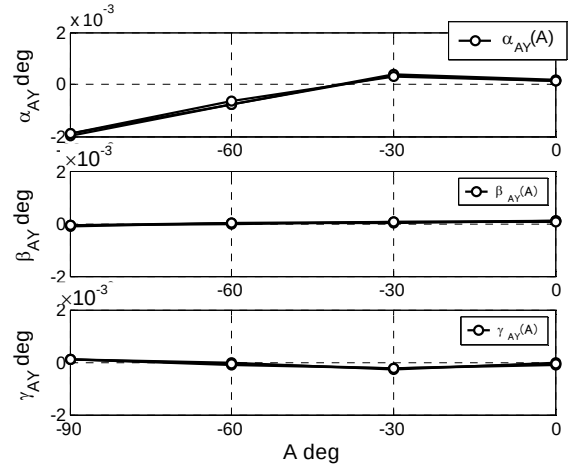

(b) $\alpha_{AY}(A_i)$, $\beta_{AY}(A_i)$, and $\gamma_{AY}(A_i)$.

Figure 7: Identified position-dependent geometric errors of A-axis, $\delta x_{AY}(A_i)$~ $\gamma_{AY}(A_i)$ for A_i=0º, -30º, -60º, and -90º.

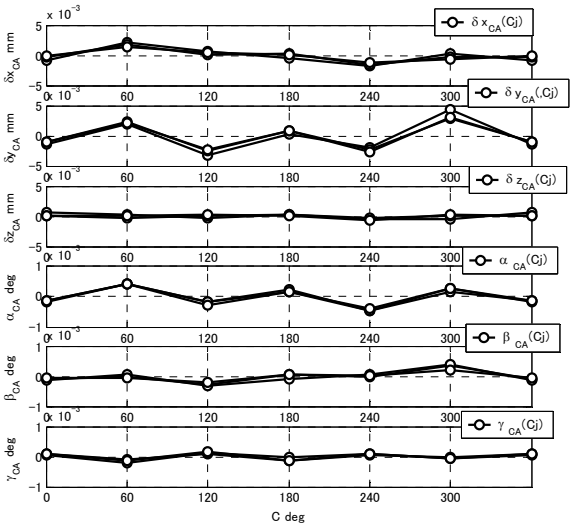

(a) At A_i=0º.

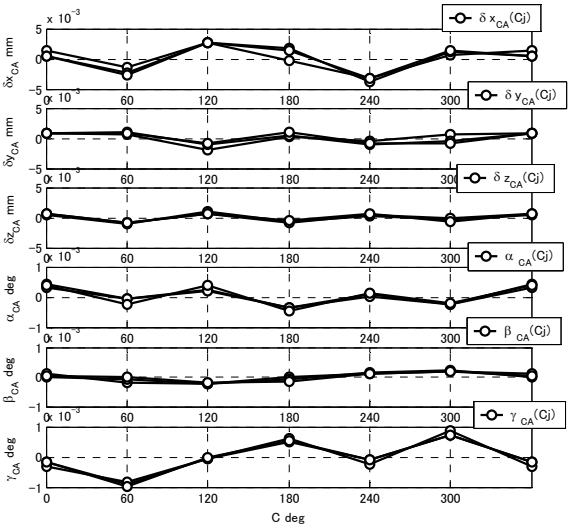

(b) At A_i=-90º.

Figure 8: Identified position-dependent geometric errors of C-axis, $\delta x_{AY}(A_i,C_j)$~$\gamma_{AY}(A_i,C_j)$ for C_j=0º~360º.

proposal for ISO standard --, *Proc. of the 7th Manufacturing and Machine Tool Conference*, pp.95-96 (in Japanese).

[7] ISO/CD 10791-6:2009, Test Conditions for Machining Centers -- Part 6: Accuracy of Feeds, Speeds and Interpolations.

[8] Schwenke, H., Knapp, W., Haitjema, H., Weckenmann, A., Schmitt, R., Delbressine, F., 2008, Geometric error measurement and compensation of machines --An update, *CIRP Annals - Manufacturing Technology*, Vol.57, No.2, pp.560-575.

[9] Veldhuis, S. C., Elbestawi M. A., 1995, A strategy for the compensations of the errors in five-axis machining, Annals of the CIRP, Vol.44, No.1, pp.373--377.

[10] Uddin, M. S., Ibaraki, S., Matsubara, A., Matsushita, T., 2009, Prediction and compensation of machining geometric errors of five-axis machining centers with kinematic errors, *Precision Engineering*, Vol.33, No.2, pp.194-201.

[11] ISO/DIS 230-10:2009, Test code for machine tools -- Part 10: Determination of measuring performance of probing systems of numerically controlled machine tools.

[12] Takeyuki Iritani, Soichi Ibaraki, Tetsuya Matsushita, 2010, "Error calibration for 5-axis controlled machine tools based on on-machine geometric measurement of artifact," *Proc. of the 2010 Spring JSPE Semiannual Meeting*, pp.1023-1024 (in Japanese).

[13] Tetsuya Matsushita, Tadahiro Oki, 2010, "Identification of Geometric Errors in Five-axis Controlled Machine Tool with Touch Trigger Probe," *Proc. of the 2010 Spring JSPE Semiannual Meeting*, pp.1105-1106 (in Japanese).

[14] Hong, C., Ibaraki, S., Matsubara, A., Influence of Position-dependent Geometric Errors of Rotary Axes on a Machining Test of Cone Frustum by Five-axis Machine Tools, *to appear in Precision Engineering*.

[15] Inasaki, I., Kishinami, K., Sakamoto, S., Sugimura, N., Takeuchi, Y., Tanaka, F., 1997, *Shaper generation theory of machine tools -- its basis and applications*, Yokendo, Tokyo (in Japanese).

[16] Renishaw website, http://www.renishaw.com